Int. J. Solids Structures Vol. 22, No. 4, pp. 445–466, 1986
Printed in Great Britain.

0020–7683/86 $3.00 + .00
Pergamon Journals Ltd.

YIELD CRITERIA BASED ON VOID COALESCENCE MECHANISMS

P. S. THEOCARIS
Department of Theoretical and Applied Mechanics, The National Technical University of Athens, 5, Heroes of Polytechnion Avenue, GR-157 73 Athens, Greece

(*Received* 30 *April* 1984; *in revised form* 11 *October* 1984)

Abstract—The mode of deformation and fracture between a pair of holes in an infinite plate submitted to uniaxial tension was studied in order to gain insight for the mechanism of ductile fracture. Void development and coalescence is accepted to constitute the basic mechanism for the creation of a cloud of defects, developed around cracks, and contributing significantly to the ductile-fracture process. The holes were considered small, in comparison to their intercentre distance, but sufficiently close to interact and concentrate slip between them. The influence of the orientation of holes on the strain state at fracture was studied for any intermediate case of loading between plane-stress and plane-strain conditions. Fracture occurred, in general, by flow localization between holes under an insignificant hole growth. The method of pseudocaustics in transmission or reflection, together with electronic scanning microscopy, proved the existence of a transition in fracture mode with the orientation of holes indicating a transition at 55°, from an intercentre necking, to an out-of-intercentre line pitting for plane-stress overall-conditions. This mode changed to a general out-of-the-intercentre-line necking for plane-strain conditions. Scanning electron microscopy indicated the mode of creation of initial hollow dimples, inside a critical area around the crack tip, and its evolution and intensification of dimple-penetration with the progress of loading. By interrelating experimental data, which support the validity of yielding criteria depending on the applied mean-normal stress and dilatancy of materials, the appropriate quantities were evaluated defining the formation and development of voids and allowed the connection of these data with modern yield criteria for ductile materials based on growth of holes.

INTRODUCTION

Failure by coalescence of microscopic voids is one of the principal mechanisms in ductile fracture. The microscopic voids engendered within the material grow, due to plastic deformation of the enveloping material, which results in a thinning of the ligaments between voids and in a successive propagation of the crack through neighbouring voids in a zig-zag path.

Gurson[1, 2] has developed a theory for studying the effect of void coalescence on the mode of failure of porous media, as this phenomenon influences the load-carrying capacity of the material.

An approximate evaluation of the critical strain for coalescence can be derived by studying models with periodic arrays of voids in various configurations[3]. Experimental evidence[4, 5] has also indicated that the critical-volume fraction of voids for initiation of the coalescence procedure is of the order of 0.05 to 0.2, which may be translated into a void-array spacing with a ligament equal to the diameter of the voids. This critical volume fraction of voids may be used as a criterion for the mode of ductile fracture. However, for the study of propagation of a crack in a ductile material a detailed description of the variation of the load-carrying capacity, localized around the instantaneous position of the crack tip, is required.

For the study of such a situation of the neighbourhood of the crack tip it is necessary to use modern yield criteria, which take into consideration plastic dilatation and eventually accepting the possibility of violation of the normality principle of the stress tensor at the yield locus. Such constitutive relations have been introduced by Mrôz[6], Rudnicki and Rice[7] and Nemat-Nasser and Shokooh[8]. Tvergaard[9,10], in a series of papers and reports, has presented a model to study the macroscopic effect of void coalescence, which was based on Gurson's model. He studied numerically the fracture mechanism by interaction of large and small voids representing the porous material. The nucleation, growth and coalescence of smaller satellite voids around the crack tip, which may be

considered as a main large void, may be studied by this type of model. He also used this model to study the development of ductile fracture in shear bands assuming a homogeneous state of deformation inside and outside the band[10].

Finally, Bourcier and Koss[11] have studied experimentally the ductile fracture of tension specimens made of different aluminium alloys, containing pairs of circular holes at different orientations. It resulted that the ductile fracture criterion is dependent on both stress- and strain-states in a complicated manner, as well as on the flow instability in the void link-up process.

In order to study experimentally the macroscopic process of void nucleation, development and coalescence, up to the point of the link-up instability in ductile fractures, a series of tests was undertaken in this paper. Pairs of holes under different orientations, modelling the situation of voids around crack tips in ductile fracture, were submitted to a tensile load up to the complete extension of plasticity in the ligament between adjacent voids. Interesting results were derived for the influence of the position and size of the holes in the mode of the ductile fracture process.

Furthermore, experience gained on the mode of void nucleation and growth around cracks and other defects was combined with empirical yielding criteria based on the influence of the mean-normal stress and the dilatancy of ductile materials. This was done in order to interpret modern criteria based on the growth of holes and yield concrete and simple relations evaluating the parameters which define such criteria.

A YIELD CONDITION DEPENDING ON PRESSURE AND DILATANCY

Classical constitutive laws assume plastic incompressibility and no effect of the hydrostatic component of stresses on yielding. However, it has been recently shown that local void nucleation and growth around the bottoms of geometric discontinuities, or the tips of existing cracks in structures, followed by a bulk dilatancy in this zone, has been observed in many cases in ductile fracture, where local plastic flow is developed. This phenomenon may play an important role on the mode of fracture in the structure[1, 2, 9, 10].

The *McClintock model*[12] of ductile fracture assumes that a mechanism of localization of deformation, starting from some discontinuity of the specimen, is developed along and within a narrow shear band, due to progressive softening of the material, by an increasing porosity. Then, the material along a zone ahead of the crack tip is damaged to such an extent that voids begin to appear with increasing load. Further loading induces the formation of a population of voids, usually in an enclave, which ultimately coalesces and initiates an extension of the crack.

It is further shown that a partial decohesion of interfaces occurs when the strength of the interface is locally attained by a local accentuation of strain-hardening, since high stresses at the interface are necessary for intergranular cavitation to begin[13].

Then, it is reasonable to accept that, while the short period of incubation of cavities is a transitional one, and does not influence directly the mode of crack propagation, the period of cavity- and void-nucleation is very important for the subsequent development of regional yielding of the material at the cavity zone, by neighbouring ligament-thinning and crack propagation.

The effect of size on fracture is incorporated in the requirement to secure a strain level over a region enclosing at least two holes, and also comprises the influence of the intercentre distance between adjacent holes, as compared to the mean diameter of the holes, the relative orientation of the holes with the main-crack axis and the direction of externally applied load.

The thickness variation is also an important factor, not only because cases vary between plane-strain and generalized plane-stress conditions, but also because the hydrostatic tension $\sigma_{kk}/3$ influences the fracture strain and especially the intermediate principal stress. Since for the validity of the process, McClintock[12] has demonstrated that all three principal stresses should be tensile for hole growth, then, if both transverse-stresses, or only one of them, is positive, this creates a big difference with the role of the intermediate principal stress, which is more important for plane-stress conditions.

Experimental evidence with scanning electron microscopy, as well as with the study of evolution of plastic zones in adjacent holes with varying orientation and varying thickness of the tensile specimen, yields ample proof of the validity of these principles.

Assuming that, for a void-containing ductile material, failure happens at some critical void volume fracture f_c, which is considerably below unity, the constitutive relations, according to the model of Gurson[1, 2], make use of an approximate yield condition of the form $\Phi(\sigma_{ij}, \sigma_m, f) = 0$, where σ_{ij} is the average macroscopic Cauchy stress-tensor, σ_m is the equivalent tensile flow stress, representing the actual macroscopic stress state in the voided matrix material disregarding local stress concentrations and f is the current void-volume fraction.

It was suggested by Brown and Embury[4] that nucleation cavities elongate along the major tensile axis and that two neighbouring cavities coalesce when their length has grown to the order of magnitude of their spacing. Then, local failure occurs by the development of slip planes between cavities, creating a necking of the ligaments. It has been estimated that critical values of the void-volume fraction may vary between 0.05 and 0.20, whereas Brown and Embury have found a value $f_c = 0.15$.

If the matrix material of the model is assumed as plastically incompressible, the nucleation of new voids is created either by decohesion of a two-phase particle–matrix material representing the model at the particle–matrix interfaces or by particle fracture. We use the void nucleation model introduced by Needleman and Rice[14], which expresses the rate of nucleation of new voids $\dot{f}_n$ by the expression:

$$\dot{f}_n = A\dot{\sigma}_m + B\dot{\sigma}_{\kappa\kappa}/3 \tag{1}$$

where A and B are real coefficients, σ_m is the effective stress as already defined and $\sigma_{\kappa\kappa}/3$ the hydrostatic stress, whereas dots mean rates with loading. This relation indicates that nucleation depends on both increments of the effective stress and the hydrostatic tension in the elastoplastic zone of loading. Indeed, the nucleation of new voids is mainly due either to decohesion between matrix and inclusions or to plastic deformation and cracking of the matrix material.

Since the matrix material is assumed plastically incompressible the increment of the void-volume fraction due to growth of voids is expressed by

$$\dot{f} = (1-f)\delta_{ij}\dot{\eta}^p_{ij},$$

where $\dot{\eta}^p_{ij}$ is the plastic part of the macroscopic strain increment. Then, the total change in the void-volume fraction is given by

$$\dot{f} = \dot{f}_g + \dot{f}_n.$$

Moreover, in Gurson's model the effective plastic strain ε^p_m in the matrix material, varying according to the equivalent plastic work expression, yields for effective stress σ_m that

$$\dot{\sigma}_m = \frac{EE_t}{(E-E_t)} \frac{\sigma_{ij}\dot{\eta}^p_{ij}}{(1-f)\sigma_m},$$

where E and E_t are the elastic and the tangent moduli, respectively.

Quantity f is the volume fraction of small-scale voids created between the larger voids, which at the beginning of loading is taken equal to zero and, as the loading is increasing, the quantity f is increasing, according to relation (1). The coefficients A and B are defined by the following relation for a material, whose void nucleation is controlled by the maximum normal stress transmitted across the interface of the matrix and inclusions[9]:

$$A = B = \frac{f_n}{s\sqrt{(2\pi)}} \exp\left[-1/2s^2\{(\sigma_m + \sigma_{\kappa\kappa}/3) - \sigma_n\}^2\right], \tag{2}$$

where σ_n is the mean nucleation stress, f_n the void-volume fraction for nucleation corresponding to the σ_n-stress and s is the corresponding standard deviation, which usually is taken equal to $s = 0.1$. Normally, for an initial value of $f_0 = 0$ the final value for f is taken to be $f_n = 0.04$ [10]. In our tests with scanning microscope in polycarbonate (PC) f_n was evaluated to be $f_n = 0.05$.

Relation (2) is valid only when the quantity $(\sigma_m - \sigma_{kk}/3)$ is an increasing function above the stress for initiation of nucleation of voids. Otherwise, the quantities A and B take the value $A = B = 0$.

Gurson[1] gave an approximate yield condition, based on an upper-bound rigid–plastic solution for spherically symmetric deformations applied around a spherical inclusion. This condition is expressed by

$$\sigma_e^2 + 2q_1 f \sigma_m^2 \cosh\left[\frac{q_2}{2}\frac{\sigma_{kk}}{\sigma_m}\right] - (1 + q_3 f^2)\sigma_m^2 = 0, \tag{3}$$

where σ_e is the macroscopic effective Mises stress, given by $\sigma_e^2 = \frac{1}{2}s_{ij}s_{ij}$ with s_{ij} the stress deviator ($s_{ij} = \sigma_{ij} - \delta_{ij}\sigma_{kk}/3$).

While Gurson[1, 2] assumed values for the constants q_i given by $q_1 = q_2 = q_3 = 1$, it was found by Tvergaard[9, 10] that a better fitting of results, for periodically arranged cylindrical voids in a matrix, with those of a continuum model is achieved, if we take that

$$q_1 = 1.5, \qquad q_2 = 1, \qquad q_3 = q_1^2 = 2.25. \tag{4}$$

Introducing these values for q_i into the yield condition (3) and denoting by f_u the ultimate void-volume fraction for which $\sigma_e = \sigma_{kk} = 0$ we obtain

$$f_u = 1/q_1 = 0.67. \tag{5}$$

For this value f_u, which corresponds to a limiting step of deformation of the body, where no more macroscopic loading can be carried by it, the value of $f_u = 0.67$ is quite high, although it is below unity. This estimation is derived from close-packed arrays of voids in a body, where this volume fraction is a limit.

Based on Tvergaard's modification of the Gurson expression for the yield criterion the current void-volume fraction f and the equivalent tensile flow stress for the voided material at the instant of initiation of plasticity were determined by considering the existing experimental data for yield criteria depending on pressure and dilatancy and adapting them to appropriate criteria. In this way oversimplifications used for the evaluation of these quantities which were based on doubly periodic arrays of circular spherical or cylindrical voids may be avoided.

THE EXPERIMENTAL MODEL

In order to study the evolution of microvoids between two relatively large voids in a ductile material, the above-sketched theory developed for ductile porous media was used to model large voids at the vicinity of the crack tip. Since the material must be taken to contain initially large voids, a pair of circular holes of a diameter $d = 2 \times 10^{-3}$ m was perforated to the initially homogeneous ductile material representing the basic unit of a periodic array of voids. As an elastic–plastic material the polycarbonate of bisphenol A (PC) was used, and simple tension specimens were prepared of varying thickness between $w = 0.75 \times 10^{-3}$ and 9.50×10^{-3} m.

The limits of the thicknesses of the perforated plates were selected to amply cover the requirements of plane-stress or plane-strain conditions. Indeed, it has been shown experimentally[15], by using the method of caustics, that for cracked plates, where the sharpness of the boundaries at the tip of the crack are of much higher curvature than for circular holes, that for thicknesses below $w = 2 \times 10^{-3}$ m plane-stress conditions are prevailing, whereas for thicknesses above $w = 15 \times 10^{-3}$ m plane-strain conditions

dominate. Then, these limits are satisfactory for our case of small holes drilled in the tension specimen.

Since we are interested in the mutual interaction of large microscopic voids during loading, the configuration of a model shown in Fig. 1 was adopted, where the angle θ of relative orientation of the axes of two neighbouring voids varies between $\theta = 0°$ and 90°. The relative position of voids and the dimensions of the specimens are indicated in this figure. In this way, six groups of specimens of different thicknesses ($w = 0.75$, 1.60, 2.00, 3.00, 4.50, 5.80 and 9.50), ranging from plane-stress to plane-strain conditions[16], with six different angles θ subtended by the loading direction and the Ox-axis of the specimen ($\theta = 0°$, 30°, 45°, 55°, 70° and 90°) were tested.

In this element, the carrying capacity of the model is reduced considerably by a failure of the ligament between the two macrovoids, which occurs by the formation of shear bands in narrow regions between the cylindrical holes and in their outer neighbourhood.

A high concentration of microvoids is developed in this zone, emanating from the interfaces of the cylinders and the matrix, which is extended progressively all over the ligament and outside the region of holes as the external loading is progressively increasing.

This is because the stress field in the hole-cluster zone is highly inhomogeneous and the local field around each hole reaches the critical yield stress at different times over the entire cross-section, so that, in the active-deformation section, certain parts are in the transformed state, whereas others are outside it.

With continuing increase of deformation, the material strain-hardens, and this reduces the amount of further deformation of the yielded zones, until the next step of a higher level of critical stress is introduced. Thus, the mode of deformation of the material around the crack tip depends solely on the relative orientation of the intercentre axes of the neighbouring to the crack tip cluster of voids from an isotropic state, to a more or less strongly oriented in a random mode, without any significant change of the overall density of the bulk of the material.

The geometry and the overall dimensions of the specimens used in the tensile tests were indicated in Fig. 1. In order to compare the results of the various tests, the applied tensile stress at the extremities of the specimens was kept always constant and equal to $\sigma_\infty =$

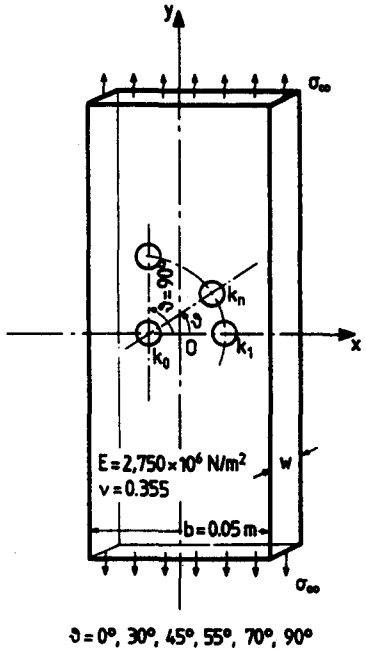

Fig. 1. The type and dimensions of the experimental model used for the study of the influence of two adjacent interacting holes, assumed lying inside the plastically deformed vicinity of a crack tip.

6.15×10^7 N m^{-2} for all orientations of the intercentre axes. This stress was 5% lower than the overall yielding of the material and it was sufficient for initiating and propagating the plastic zones around the holes. Indeed, all plastic zones were fully developed after a period of constant loading of the specimens of 5–8 min. It was observed that after the lapse of these time intervals and for the slowly applied increments of loads applied to the specimens, no detectable creep phenomena appeared in the vicinity of the perforations of the specimens.

For the detection and evaluation of the plastic zones developed in the vicinity of the holes the method of reflected caustics was used. The principle of the method and the experimental setup are fully described in Ref. [17].

Figure 2 presents a series of photographs of the caustics formed along the plastic zones, developed either along the ligament between the adjacent holes or outside this ligament zone, for various angles θ of orientation of the two holes.

It may be immediately observed that the plastic zones present a bottom line of maximum contraction, which is always a sigmoid curve, intersecting the intercentre axis at its middle. Plastic protrusions are also developed at the rims of the holes, so that the bottoms of plastic ravines are angularly displaced by an angle $\Delta\theta$, varying between 10 and 18 degrees with the intercentre axis, towards the loading axis.

Figure 3 presents the variation of angle $\Delta\theta$ between the intercentre axes and the bottoms of the plastic ravines versus the angle θ of orientation of the pair of holes. It is clear from this figure that the angle $\Delta\theta$ increases rapidly to a constant limit of 18 degrees, as θ is increasing from zero to 50 degrees and then drops abruptly to zero.

Indeed, for an angle θ of 50–55°, the mode of plastic deformation in the ligament between holes changes drastically. Below 50° there is always for all specimens from plane-stress conditions (thickness $w = 0.75 \times 10^{-3}$ m) to fully plane-strain conditions ($w = 9.50 \times 10^{-3}$ m) a plastic zone developed between holes. Above this limit of the θ-angle, the plastic deformation of all plates changes mode, presenting only typical plastic asymmetric zones on both sides of each hole, which develop independently, without coalescence in the ligament between holes. These squid-like plastic zones extend to different lengths, and unsymmetrically on both sides of the central part of holes, forming an angle with the respective radial directions. The regions of their emergence from the rims of the holes are extended about the transversal axes of the holes, and their length passes through a minimum, for angles θ between 20 and 45°, because in this region of angles θ plastic deformation is mainly concentrated in the ligament between holes. Above $\theta = 45°$, these external plastic zones are progressively increased at a direction of approximately 45° to the longitudinal axis of the specimen.

This phenomenon of change of mode of the development of plastic enclaves around the pair of holes remains unchanged, if the thickness of the specimens is increased and the state of deformation of the plate changes from plane-stress to plane-strain.

The extent of plastic deformation in the ligament zone as well as in the outer zones was studied by defining the topography of the deformed lateral faces of the plates. For this purpose use was made of a *rectilinear surface graph-recorder* of the type of Talysurf No. 4. The instrument has a very fine stylus, which scans the surface of the test piece along lines normal to the apparent axis of maximum plastic deformation. The area surrounding the pair of holes was scanned and Fig. 4 presents the profile graphs of rectilinear traverses parallel to the loading axis of the specimen for three different angles ($\theta = 0°$, 30° and 45°) and for a thickness $w = 0.75$ mm. It is clear from this figure that the bottom lines of the plastic zones between holes are sigmoid curves and their maximum depths appear at the close vicinities of the rims of the holes.

Figure 5 presents the variation of depth of the plastic zones for three different specimens with thicknesses $w = 1.54$, 1.66 and 2.00 mm, respectively, as they have been evaluated from the respective profile graphs. It is interesting noting that the larger depths in plastic zones appear very near the rims of the holes and at distances of the order of 0.1 mm from these rims. These are the zones where clouds of voids are developed when the critical loading for void formation is attained.

Another relative minimum, in the form of a valley, appears always at middistance

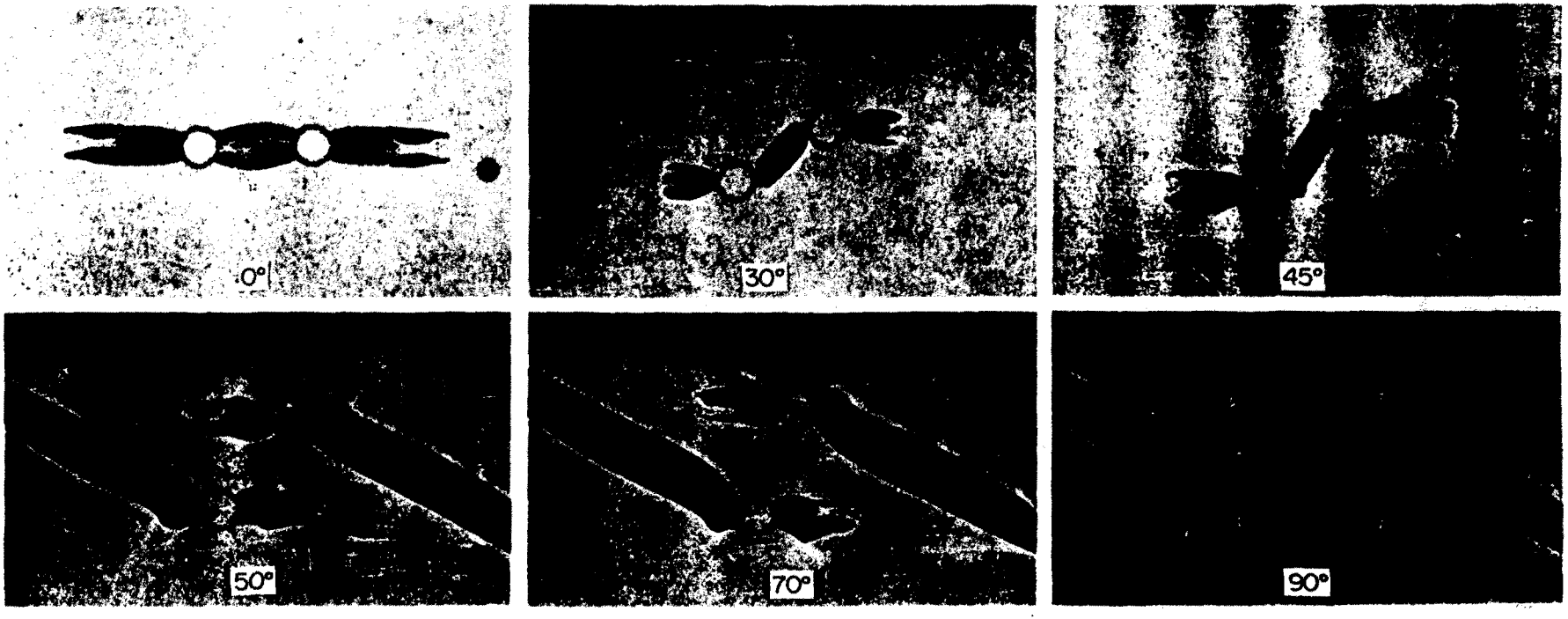

Fig. 2. Series of photographs of transmitted caustics developed at the intercentre zone and the outer neighbourhood of two interacting holes lying inside the plastic zone developed around the tip of a crack for various orientations of their intercentre axis.

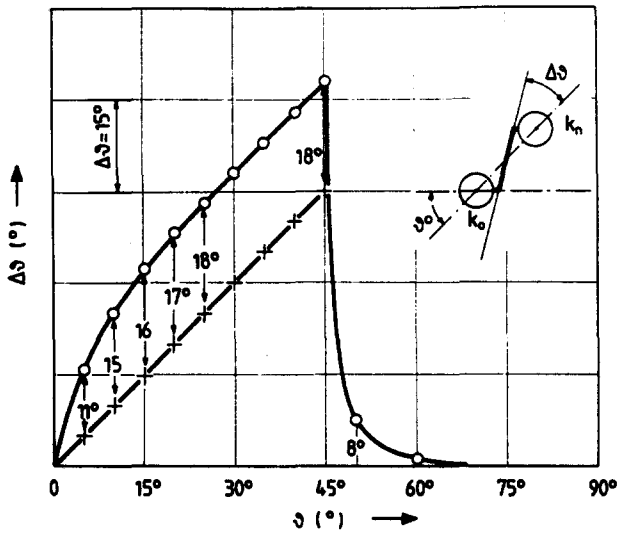

Fig. 3. The variation of the difference $\Delta\theta$ between the orientation angles of the bottom lines of the plastic zones and the respective intercentre line of two adjacent interacting holes under various orientations.

between holes. While for $\theta = 45°$ the absolute minima approach the rims, their absolute depths are decreased in comparison with the topography of the plastic zone for $\theta = 0°$.

Figures 6 and 7 present the percentage reductions of the thickness of the specimens at the rims of the holes and at the zones of the inner and outer maxima of plastic deformation, for the various thicknesses w of specimens tested and different angles θ of orientation of the holes.

The experimental results presented in the last three figures were obtained by loading all specimens with constant stresses at infinity and equal to $\sigma_\infty = 6.15 \times 10^7$ N m^{-2}. This stress corresponds to an elastic loading creating stresses 5% below the yield limit σ_0 of the material in simple tension. In this way the overall development of the plastic enclaves around the pair of holes corresponded to identical loading configurations of the plates and therefore the experimental evidence was comparable.

It is clear from these figures that, for typically plane-stress specimens (thicknesses below $w = 1.5$ mm), the plastic maxima are very high for all angles θ, whereas for prevailing

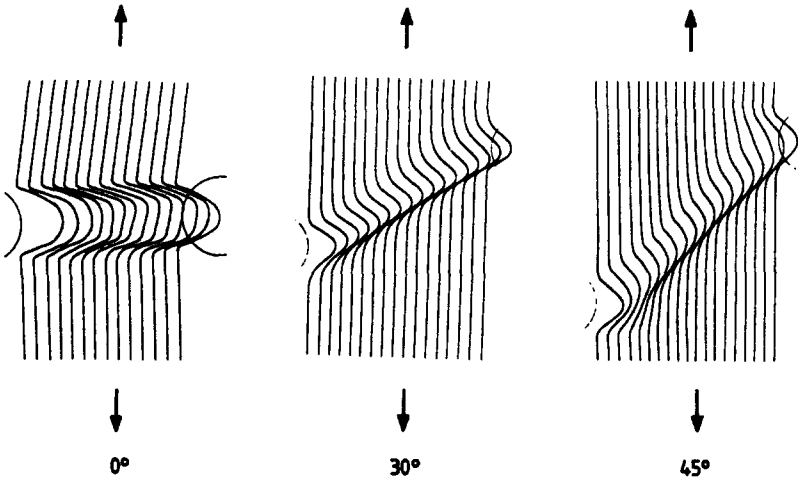

Fig. 4. The depth-profile graphs of the intercentre regions between adjacent interacting holes submitted to a tensile load for different orientations of the intercentre lines of holes ($\theta = 0°$, 30° and 45°). The scanning traverses were executed in a direction almost parallel to the loading axis of the specimens.

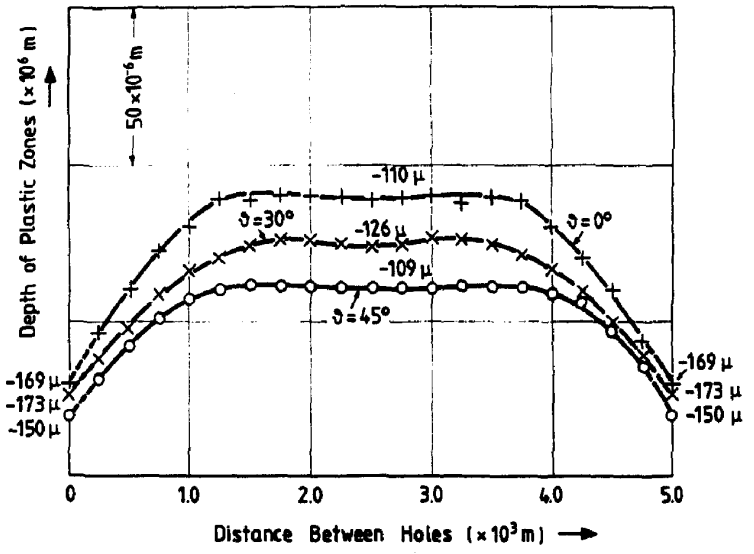

Fig. 5. The variation of the depth of the plastic zones developed at the intercentre zones of specimens containing a pair of interacting holes for $\theta = 0°$ and three different thicknesses of the plates (w = 1.54, 1.66 and 2.00 mm, respectively).

plane-strain conditions (w = 9.5 mm), these maxima are insensitive to the angle θ and very low.

This fact has as a result to make plane-stress specimens more prone for developing large plastic deformations at the vicinity of holes and therefore to facilitate the development of clusters of voids in front of the crack tips. This phenomenon makes such specimen easy to follow the mode of fracture by void coalescence.

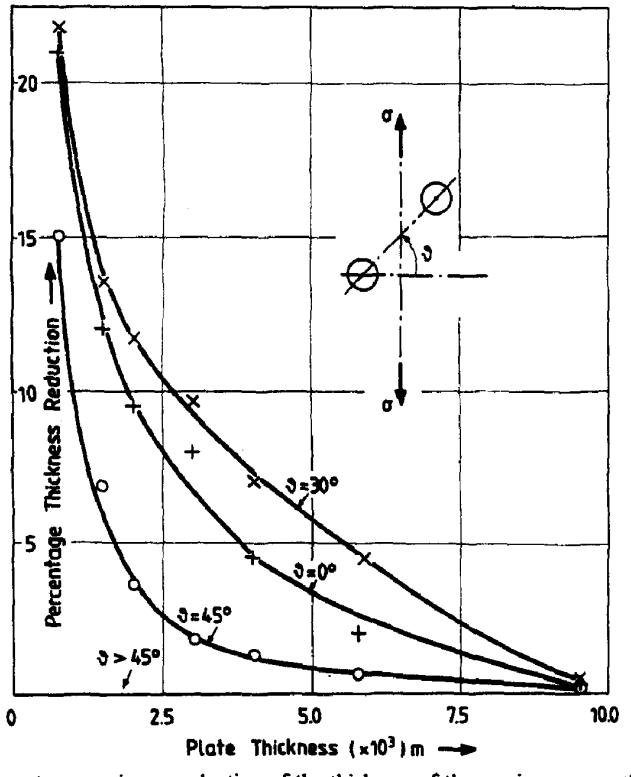

Fig. 6. The percentage maximum reduction of the thickness of the specimens near the rims of the holes and the intercentre line versus the thickness of the specimen for different angles of inclination of the intercentre line.

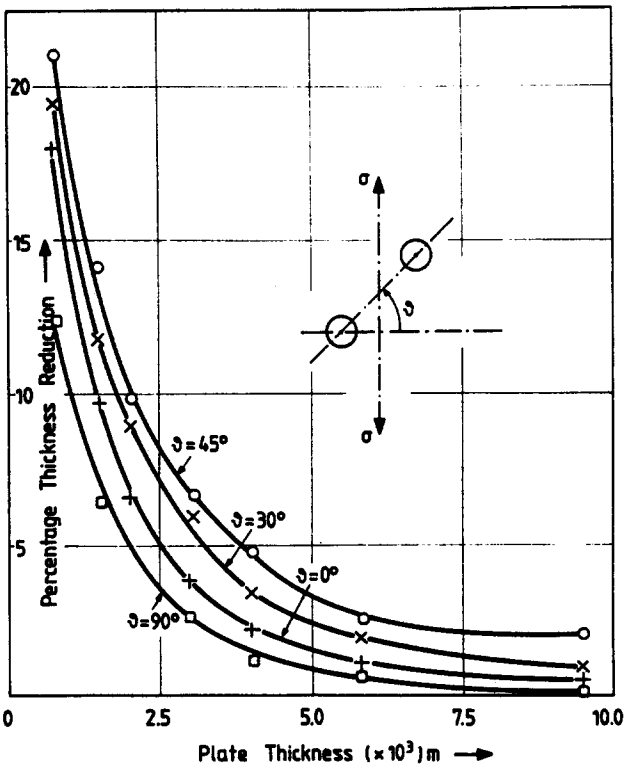

Fig. 7. The percentage maximum reduction of the thickness of the specimens at the plastic zones developed outside the intercentre zone between holes versus the specimen thickness for different angles of inclination of the intercentre line.

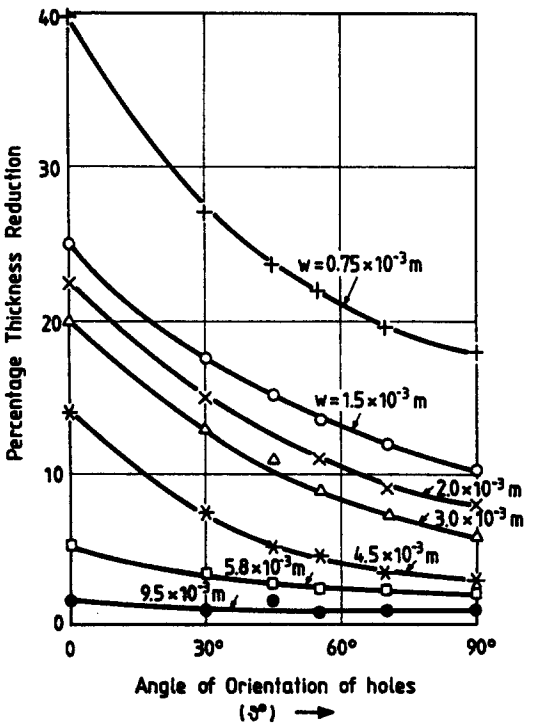

Fig. 8. The percentage maximum reduction of the thickness of the specimens at the plastic zones outside the intercentre zone between holes versus the angle of orientation of the holes for different parametric values of the thickness of the specimen, from plane-stress to plain-strain conditions.

Figure 8 presents another aspect of the amount of plasticity in the outer squid-like zones by plotting the real maximum values of plastic outer enclaves at a distance 0.5 mm from the rims of the holes, versus the angle θ of orientation of the holes for different parametric values of the thickness w of the specimens. These maximum values are much higher than the corresponding relative maxima percentage-depths, appearing at the rims of the holes and presented in Figs. 6 and 7. Although all specimens were loaded with identical overall tensile stresses at infinity, the shapes, forms and sizes of the plastic zones were different, depending on the particular characteristics of each configuration of the holes. Again the typical influence either of the thickness of the specimens or the angle θ is clearly demonstrated.

While Fig. 2 presents the dependence of the development of plastic zones between two neighbouring macrovoids, Figs. 5–8 give ample experimental evidence of the forms and depths of plastic zones between neighbouring voids and their dependence on their relative orientation with respect to the crack and loading axes, as well as on the thickness of the specimen, which defines the particular stress conditions (plane stress or plane strain) holding either along the intercentre distance between neighbouring holes or outside their intercentre zone.

Then, these figures exemplify the different modes of creation of furrows between neighbouring voids, which are the precursors of an eventual propagation of the nearby existing crack, which follows one of these ravines.

From this experimental study of a typical arrangement of a pair of holes developed at the neighbourhood of the tip of a crack in a plate, it may be concluded that all voids developed in this vicinity participate in the fracture mechanism of the plate. Those, which are relatively oriented with angles θ smaller than 55°, create plastic bridges between them, which, later on, evolute and create probable paths of crack propagation by kinks.

The voids which form between them angles greater than 55° develop squid-like external plastic enclaves, which are oriented almost parallel to the crack axis and may coalesce with neighbouring voids in the near cluster of voids. These voids also facilitate the prospective extension of the crack since they create transverse bridges between neighbouring voids.

This kind of deformation is developed in voided plates under uniaxial tensile loading at the zone of the cloud of voids. However, since the elastic- and plastic-stress fields in front of a crack are, in general, biaxial for plane-stress, or triaxial in the general case, the intermediate component of stress in the plane of the plate contributes significantly to the mode of crack propagation by providing an additional stress field of smaller intensity, but oriented by 90° to the main σ_y-stress field. It also participates in the development of voids in regions, where the main field because of orientation ($\theta \geqslant 55°$) cannot create plastic ligaments between adjacent voids, provided it is an overall tensile field.

Although the experimental evidence presented in the previous figures is based on the plastic straining of a glassy polymer, qualitatively the same phenomena are expected to appear for crystalline metallic specimens, provided that the mode of fracture of the prototypes and the model are the same. Furthermore, there is extensive experimental evidence in the literature that polycarbonate behaves like mild steel and may be used as a substitute for the study of plastic straining of elastic–perfectly plastic materials, although the author, in a previous publication, demonstrated existing differences between these two different types of materials[18]. However, for the qualitative description of the phenomenon of fracture by void creation around the loaded crack tip and void coalescence, the use of the polycarbonate model gives a satisfactory picture constituting macroscopically a parallel phenomenon as those in crystalline substances.

This explanation corroborates the findings of McClintock, who has introduced the condition that the holes should remain open during loading and thus fracture by hole growth occurs always after necking of a tensile specimen[15]. The necessity of ellipticity of the holes implies the dependence of yielding and fracture on the mean-normal stress, and especially its strong dependence on the intermediate principal stress.

The formation of shear bands between holes suggests that the link-up mechanism between voids is dominated by shear stresses. Similar examples are reported in Ref. [11] for aluminium alloys, which resemble classical microphotographs on other aluminium and steel

plates. Examination of the fracture surface profiles in these examples indicate, indeed, that in the ligaments between holes fracture occurs at angles $\theta \leqslant 60°$. Moreover, the profiles of the substrata of the plastically thinned ligaments between holes deviate successively on both sides of the intercentre lines in the form of sigmoid curves, reminiscent of the respective slip-line fields and indicating a progressive influence of the plastic deformation between adjacent voids[19].

EVALUATION OF VOID POPULATION AT THE CRACK TIPS

We have studied the mechanism of ductile fracture, developed by the McClintock–Gurson model of localization of deformation inside shear bands. These bands are developed because of the softening process of the material, by increasing its porosity due to void growth. We try now to evaluate, by scanning microscopy, the extent of this porous region.

For this purpose standard 1-mm-thick dogbone specimens, made of PC and suitable for insertion in the loading chamber of the scanning electron microscope, were prepared and duly coated to reflect the electron bundle impinging on their surface. With this arrangement and coating of the surfaces the plastic zones developed around the crack tip were clearly apparent as illuminated surfaces, because of the intense reflection of the electrons in these zones. The remaining part of the specimen remained obscure, because of the infinitesimal elastic stress field there.

By a proper selection of the magnification factor in the SEM, the plastic enclave during loading was always inside the field of view of the microscope. The holes were developed in the plastic zone when the tensile load was slowly increasing under isothermal conditions in the loading chamber. A number of holes started to develop on the surface of the specimen and very rapidly tended asymptotically to the limiting population of holes in the plastic zone for impending development of a kink in the crack. A typical curve of the increase of the void surface versus applied tensile stress on the specimen is given by the graph of Fig. 9. The limiting stress of 5×10^7 N m^{-2} applied to the specimen was at the threshold of crack initiation. Similar curves have been given by Gurson in his Fig. 3 of Ref. [2].

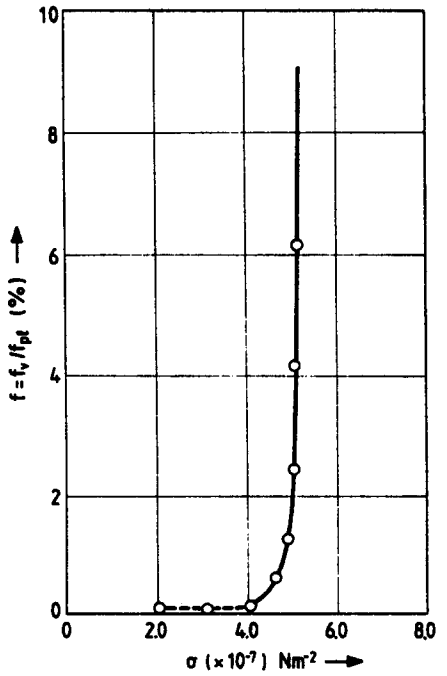

Fig. 9. The evolution of the volume void-fraction f, expressed as the ratio of the volume surface, f_v, covered by voids, normalized to the size of the plastic zone f_{pl} around the crack tip versus the externally applied σ-stress of a cracked specimen made of PC.

From a series of such plots it may be safely derived that the area covered by voids S_v on the surface of the specimen does not exceed 5% of the respective plastic enclaves S_{pl}, which are generally of the order of $S_{pl} = 5 \times 10^{-3}\,\text{mm}^2$. The average number of voids from the electron photographs was equal to 30 in the range of surface S_{pl}. Then the surface covered by the voids was $S_v = 2.5 \times 10^{-4}\,\text{mm}^2$ with an average radius $R_v = 1.7\ \mu\text{m}$. Assuming that the shape of voids is approximately spherical and their density inside the specimen follows a similar distribution as in the surface, we may readily define that the void volume f_v is approximately $7 \times 10^{-5}\ \text{mm}^3$. This volume, compared to the plastic-enclave volume $f_{pl} = 5 \times 10^{-3}\,\text{mm}^3$, yielded a volume density of voids in the plastic zone equal to

$$f = \frac{f_v}{f_{pl}} = 0.014. \tag{6}$$

Figure 10 presents a series of electron micrographs taken with the z-modulation arrangement, which indicate the topography of the plastic zones around the progressing crack tip and the position and size of the voids developed in this zone. It is clear from this series of photographs that, at the beginning, a small number of surface voids are developed. As the loading is increasing the number of voids increases rapidly to some limit and simultaneously their depth is increased considerably, especially at the vicinity of the crack tip and flanks.

It is interesting to observe that, while their shape on the lateral face of the specimen is approximately circular, tending to elliptic, when they penetrate inside the specimen they take conical forms. This is a clear indication that inside the thickness of the specimen in the plane-strain zone the void density is drastically reduced from the density at adjacent layers to the surfaces. Then, the void distribution, based on calculations of the surface-void population, constitutes an upper limit. The real void population should be much smaller, and it is reasonable to reduce the above figure in relation (6) to

$$f = 0.01. \tag{7}$$

EVALUATION OF THE VOLUME VOID FRACTION f DIFFERENT LOADING CONDITIONS

The void population inside the plastic zone around the crack tip depends on the state of stress at each point. Then, it is important to calculate the stress distribution around the crack in order to define $f = \phi(\theta)$.

We interconnect now the phenomena appearing in the microscale by the process of void initiation, growth and coalescence in the plastic zone around the crack tip, with the resulting functional dependence of the yield and fracture criteria on the stress- and strain-distribution around the crack tip. Without making recourse to any approximate models we simply accept that, since void nucleation and development are the main factors for creating differences in the yield loci of ductile materials at their different stress quadrants, we directly interrelate yield loci depending on the mean-normal stress and dilatancy with the characteristic parameters defining the influence of voids.

According to McClintock's model, it is entailed that the initiation of fracture is governed by the requirement that the holes created around the crack tip during loading remain steadily open, so that the damage rate there is always positive[1,12]. This necessitates that the stress field around each hole remains extensional and especially the mid-principal stress remains positive. This fact implies that the process of nucleation and development of holes strongly depends on the position of the stress field in the (σ_1, σ_2)-stress diagram (for plane stress or strain conditions). Indeed, while in the first (σ_1, σ_2)-quadrant the evolution of voids is intense, in the fourth quadrant, where a compression–compression state of stress dominates the rate of creation of voids is expected to be either zero (at 215°) or very limited.

Since all yielding criteria assume isotropy in tension and compression and symmetry

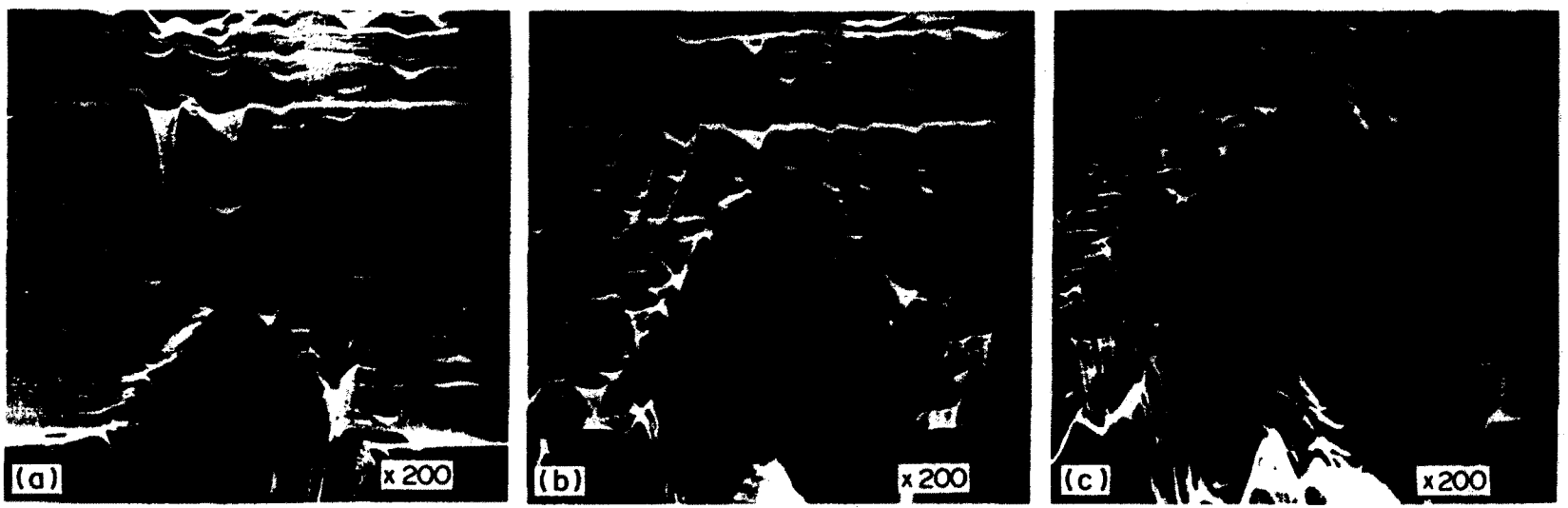

Fig. 10. A series of scanning electron micrographs, taken with z-modulation arrangement of the apparatus, and indicating the population of voids developed in the plastic zones around the crack tip of an increasingly loaded specimen.

of the yield loci, they neglect an important factor, due to the stress differential effect, where $\sigma_{0c}/\sigma_{0t} = R > 1$ for all materials.

Then, it is reasonable for a better understanding of the mechanism of void nucleation and development to make recourse to more accurate yield criteria, which take into consideration the effect of the difference of yield stresses in simple tension (σ_{0t}) and compression (σ_{0c}).

The use of such criteria, instead of the classical yield loci, is also implicitly imposed by the fact that these criteria contain always a term depending on the first stress invariant, J_1, which is the dominating factor regulating the rate of creation and evolution of voids.

Two main quantities should be defined for the complete determination of the yield locus based on the McClintock–Gurson model, that is the threshold stress, σ_m, of initiation of the cavitation phenomena and partial decohesion of interfaces of grains, which occur when the strength of the matrix material, without voids, attains locally the strength of the interface, and the void-volume fraction, f, as a function of the existing local state of stress at each point in the neighbourhood of the crack tip. This means that the σ_m-stress must equal the yield stress of the material in biaxial compression when presumably no void can be created and the void-volume fraction must be a function of the θ-polar angle in a (σ_1, σ_2)-stress diagram.

Much experimental evidence has shown that various empirical yield criteria depending (besides on the second stress invariant J_2 or in general on shear stressing) on the first stress invariant, J_1, expressed by the sum of principal stresses are more suitable for describing accurately the yielding behaviour of most of the materials used in the applications. For a review of the validity of these criteria, see Refs. [20, 21].

There is a series of criteria which take into consideration the differential strength effect, where the yield stress in simple tension, σ_{0t}, is different than the yield stress in compression, σ_{0c}. Then the ratio $R = \sigma_{0c}/\sigma_{0t}$ is always different than unity and normally higher. Among them, the most popular are the Schleicher–Stassi criterion[22, 23], which for plane stress conditions is expressed by

$$3J_2 + (\sigma_{0c} - \sigma_{0t})J_1 = \sigma_{0t}\sigma_{0c} \tag{8}$$

in which the J_2-invariant in the first left-hand side term expresses the typical Mises criterion and the second term incorporates the influence of the first stress invariant J_1. These invariants are given by

$$J_1 = \sigma_{\kappa\kappa} \quad \text{and} \quad J_2 = \tfrac{1}{2}s_{ij}s_{ij} = \tfrac{1}{2}(\sigma_{ij} - \delta_{ij}\sigma_{\kappa\kappa/3})(\sigma_{ij} - \delta_{ij}\sigma_{\kappa\kappa/3}). \tag{9}$$

The right-hand side term replaces the typical squared yield stress in simple tension σ_{0t}^2 by the geometric mean of the yield stresses in simple tension and compression $(\sigma_{0t}\sigma_{0c})$. The rival criterion to the Schleicher–Stassi criterion is the Nadai–Bauwens–Sternstein criterion, which for plane-stress conditions may be expressed in the form[24–26]

$$\left(\frac{\sigma_{0c} + \sigma_{0t}}{\sqrt{2}}\right)(J_2)^{1/2} + (\sigma_{0c} - \sigma_{0t})J_1 = 2\sigma_{0t}\sigma_{0c}, \tag{10}$$

where J_1 and J_2 are again the first and second stress invariants.

From the structure of the two types of criteria shown in relations (8) and (10) it may be definitely concluded that criterion (8) is more sound. Indeed the individual terms of relation (8) correspond the first term to a distortional component of energy, the second one expresses some kind of dilatational energy since the hydrostatic component of stresses is multiplied by a normal stress equal to the difference $(\sigma_{0c} - \sigma_{0t})$ and finally the third term on the right-hand side of eqn (8) replaces the corresponding energy due to simple tension.

On the contrary, the first left-hand term of eqn (10) does not represent any kind of distortional energy component and therefore creates some kind of confusion in the energy terms entered in the criterion.

On the other side, it can be readily shown that for values of a strength-difference coefficient $R = \sigma_{0c}/\sigma_{0t}$ approaching $R = 3.0$, that is where the materials become progressively more and more brittle, the deviations between the two types of criteria increase rapidly and the Nadai–Bauwens–Sternstein (NBS) criterion becomes unlimited in the compression–compression zone, whereas the respective Schleicher–Stassi (SS) criterion is expressed always by a typical elliptic locus. Figure 11 presents the evolution of the two criteria as R is increasing and takes values $R = 2.0$, 3.0 and 4.0. Dotted lines in Fig. 11 correspond to the NBS criterion, whereas the full line for $R = 3.0$ corresponds to the SS criterion.

Experimental evidence with cast-iron specimens with $R = 3.0$, executed as early as 1949 and 1950, proves the validity of the SS criterion. In the same figure some experimental points taken from Grassi and Cornet[27] and from Coffin[28] were plotted indicating the coincidence of the NBS criterion with experimental evidence.

On the other hand, it is worth indicating that the NBS criterion incorporates the Mohr–Coulomb criterion for brittle materials as it stands to date, although again this very old criterion needs some modifications to reconcile it with the fact of existence of failure in compression–compression zone even for the brittle materials.

Based then on a large experimental evidence of the validity of the SS criterion for the whole spectrum of ductility or brittleness of materials[21], we evaluate first the σ_m-equivalent tensile flow stress of the voidless matrix material by assuming that in the compression–compression zone of loading with $|\sigma_1| = |\sigma_2|$ the real yielding value of stress corresponds to the σ_m-stress. Then, for various values of the stress-differential parameter R we evaluate the respective σ_m-stress for the points of the respective loci where $(-\sigma_1) = (-\sigma_2)$. Figure 12 presents the variation of the σ_m-stress versus the differential-stress parameter R in the interval between $R = 1.0$ (complete ductility) and $R = 6.0$ (high brittleness). This curve appears to be a straight line.

In order to evaluate the variation of the void-volume fraction at the initiation of yielding for any combination of the components of stresses in the (σ_1, σ_2)-plane we define the particular value of R for the material under study. We assume valid the relation (8) expressing the SS criterion (in the case when the material obeys the NBS criterion we use relation (10) instead of (8)), and we introduce to it the value of R and the polar expressions for the stresses σ_1 and σ_2 defining the respective yield locus. In this case relation (8)

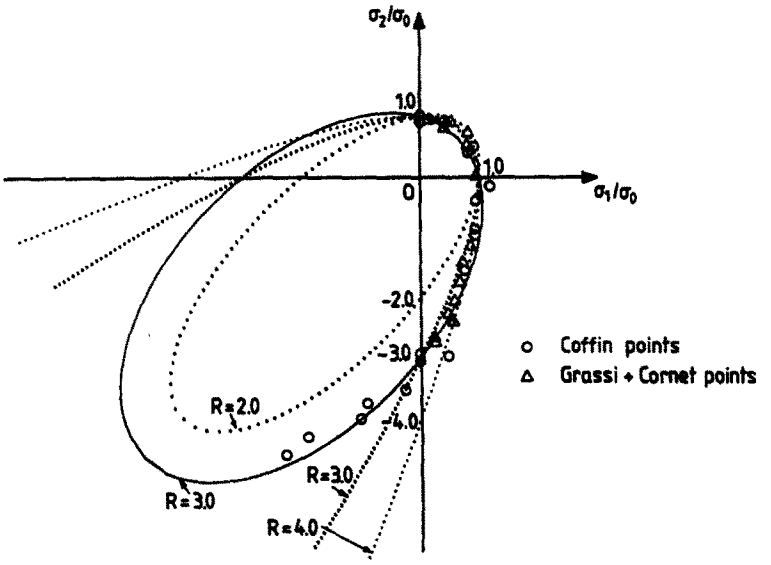

Fig. 11. The family of the yield loci for the Nadai–Bauwens–Sternstein criterion with the stress-differential coefficient R varying between $R = 1.0$ and $R = 4.0$ plotted in the (σ_1, σ_2)-plane for plane-stress conditions and the respective yield locus for the Schleicher–Stassi criterion for $R = 3.0$ together with experimental evidence with cast-iron specimens ($R = 3.0$).

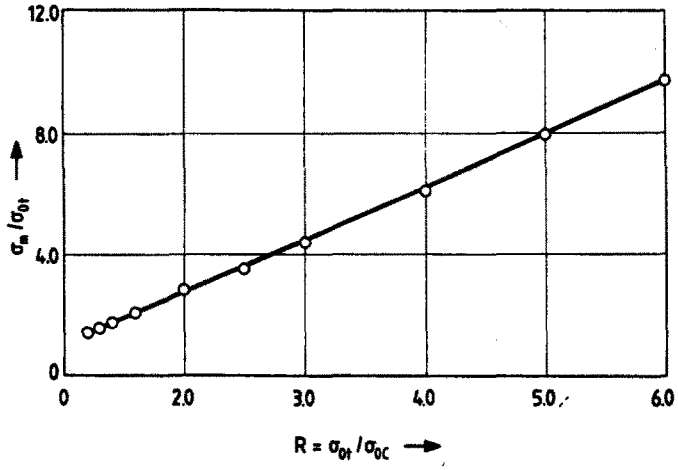

Fig. 12. The variation of the σ_m-equivalent tensile flow stress in the matrix material, disregarding local stress variations due to voids, versus the stress-differential parameter, R, for a series of materials from ductile ($R = 1.0$) to brittle ones ($R > 5.0$).

becomes

$$\rho^2\left(1-\frac{\sin 2\theta}{2}\right)+\sigma_{0t}(R-1)\rho(1+\sin 2\theta)^{1/2} = R\sigma_{0t}^2. \tag{11}$$

Solving relation (11) for θ's varying between zero and 2π we define the values of ρ corresponding to each value of the polar angle θ and from these values of ρ the corresponding values of the σ_1- and σ_2-components of stresses for yielding ($\sigma_1 = \rho \cos\theta, \sigma_2 = \rho \sin\theta$).

Introducing now the pairs of stresses corresponding to each value of θ and ρ into eqn (3) we obtain a relationship between σ_m and f.

For the value of σ_m corresponding to the respective value of R, defined from the graph of Fig. 12, and limiting ourselves to solutions for positive f's we derive from eqn (3) a relationship $f = \phi(\theta)$ of the variation of the void-volume fraction at the initiation of yielding versus the polar angle θ. Figure 13 presents the variation of the void-volume fraction for

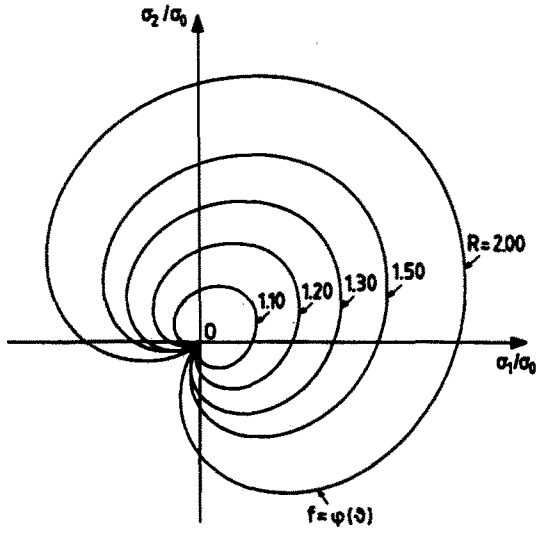

Fig. 13. The variation of the void-volume fraction for initial yielding, f, around a crack tip versus the polar angle θ in the (σ_1, σ_2)-plane for parametric values of the stress-differential parameter, R, between $R = 1.0$ (ductile materials) and $R = 2.00$ (semibrittle materials).

initiation of yield versus the polar angle θ in the (σ_1, σ_2)-stress plane for values of the stress-differential parameter R varying between $R = 1.0$, corresponding to perfect ductility, and $R = 2.00$ for quasi-brittle materials.

It is clear from this figure that for $R = 1.00$ the $f = \phi(\theta)$ curve is degenerated into one point coinciding with the origin of coordinates in the (σ_1, σ_2)-plane. For values of $R > 1.00$ cuspoid curves are developed presenting a zero value for $\theta = 5\pi/2$. Indeed for this point which corresponds to a compression–compression state of stress at the element of the specimen the void formation should be equal to zero.

On the other hand, the state of maximum void formation appears at $\theta = \pi/4$, where $\sigma_1 = \sigma_2$ and both are positive thus increasing isotropically the size of voids without distorting their shape.

Moreover, there are zones where both principal stresses may be negative and, contrary to what is believed up to now, voids may be developed under such modes of stressing of the elements. However, these lobes of both negative principal stresses are limited zones in the diagrams $f = \phi(\theta)$ and they increase in size as R and therefore brittleness is increasing.

Whereas all loci of $f = \phi(\theta)$ corresponding to initial yielding for every value of the stress-differential parameter, R, of the material present a cusp point coinciding with the origin of the (σ_1, σ_2)-coordinates, for subsequent loading beyond the initial yielding, that is for higher values of σ_m than the σ_m^0-value for initiation of yielding, the $f = \phi(\theta)$ curves, although they maintain their overall shape as quasi-cardioid curves, their blunted cusps do not anymore coincide with the origin of the coordinates, but they recede from this point as the values of σ_m increase.

Figure 14 presents the variation of the void-volume fraction f around a crack tip, versus the polar angle θ in the (σ_1, σ_2)-plane for $R = 1.3$ and initial yielding $\sigma_m = 1.50\sigma_{0i}$ and subsequent extensions of yielding corresponding to values σ_m/σ_{0i} between 1.70 and 2.50. These shapes of cardioid curves indicate that, as plasticity is progressing negative, also values for both principal σ_1- and σ_2-stresses may develop voids and participate in the plastic deformation of the solid by void nucleation and overall dilatation of the zone surrounding the crack tip.

CONCLUSIONS

In this paper the strong influence of voids on the onset of plastic ligaments, in the vicinity of the tip of a crack submitted to mode-*I* deformation, was studied on the basis of

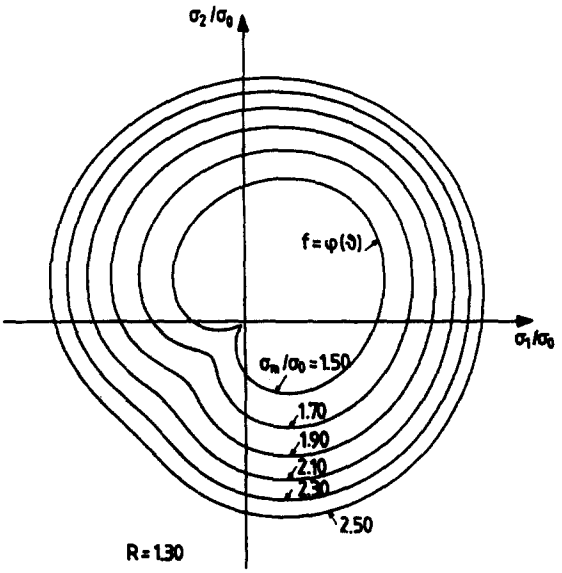

Fig. 14. The variation of the void-volume fraction, f, around a crack tip versus the polar angle θ in the (σ_1, σ_2)-plane for $R = 1.30$ and various steps of loading corresponding to σ_m between $\sigma_m/\sigma_{0i} = 1.50$ and $\sigma_m/\sigma_{0i} = 2.50$.

a model consisting of two equal holes with their intercentre axis oriented to different angles with respect to the loading axis.

The mechanisms of the development of plastic enclaves in the ligament between holes, as well as outside it, were studied and critical angles of orientation were established, at which one mechanism of plastic deformation changes to another. The influence of thickness of the specimen and the stress conditions of the plate was studied and the change of deformation mode from plane-stress to plane-strain conditions graphically indicated.

A simplified physical model was used for establishing a quantitative formulation for the McClintock–Gurson yield and fracture criterion, based on the growth and coalescence of existing voids developed in the plastic zones created at the vicinity of crack tips. By comparing the yield condition for the voided material with experimental evidence of various materials presenting the stress-differential effect, and the respective macroscopic yield condition, the maximum nominal traction, σ_m, for a certain void content influencing the mode of yielding of the ductile material was defined, related to the respective yield stress for a compression–compression state of stress, when presumably the amount of voids is minimized.

Furthermore, by comparing the yield loci for the respective stress-differential effect of the material studied with the characteristic quantities involved in the voided-material yield condition, the critical dependence of the void-volume fraction, f, as a function of any combination of state of stress in the plate was established. This function allowed the complete definition of the voided-material yield locus, without making recourse to any approximating models, where arrays of spherical or cylindrical holes are considered in a convenient population density.

Acknowledgement—The author is indebted to his assistant Dr. Costas Stassinakis for helping him in the computer calculations involved in this research project.

REFERENCES

1. A. L. Gurson, Continuum theory of ductile rupture by void nucleation and growth—Part I. Yield criteria and flow rules for porous ductile media. *J. Engng Mater. Technol.* **99**, 2–15 (1977).
2. A. L. Gurson, Porous rigid-plastic materials containing rigid inclusions—yield function, plastic potential and void nucleation. In *Proc. 4th Int. Conf. Fracture* (Edited by D. Taplin), Vol. 2A, pp. 357–364. Pergamon Press, Elmsford, New York (1977).
3. A. Needleman, Void growth in an elastic–plastic medium. *J. Appl. Mech.* **39**, 964–970 (1972).
4. L. M. Brown and J. D. Embury, The initiation and growth of voids at second-phase particles. In *Proc. 3rd Int. Conf. on Strength of Metals and Alloys*, pp. 164–169. Inst. of Metals, London (1973).
5. S. H. Goods and L. M. Brown, The nucleation of cavities by plastic deformation. *Acta Metal.* **27**, 1–15 (1979).
6. Z. Mróz, On forms of constitutive laws for elastic–plastic solids. *Archwm. Mech. Stosow.* **18**, 3–35 (1966).
7. J. W. Rudnicki and J. Rice, Conditions for the localization of deformation in pressure-sensitive dilatant materials. *J. Mech. Phys. Solids* **23**, 371–394 (1975).
8. S. Nemat-Nasser and A. Shokooh, On finite plastic flows of compressible materials with internal friction. *Int. J. Solids Structures* **16**, 495–514 (1980).
9. V. Tvergaard, Ductile fracture by cavity nucleation between larger voids. *J. Mech. Phys. Solids* **30**(4), 265–286 (1982).
10. V. Tvergaard, Material failure by void coalescence in localized shear bands. *Int. J. Solids Structures* **18**, 659–672 (1982).
11. R. J. Bourcier and D. A. Koss, Ductile fracture under multiaxial stress between pairs of holes. In *Proc. Fifth Int. Congr. Fract., Cannes, France 1981* (Edited by D. François), Vol. I, pp. 187–194. Pergamon Press, Oxford (1981).
12. F. A. McClintock, A criterion for ductile fracture by the growth of holes. *J. Appl. Mech. Trans. ASME* **35**(2), 363–371 (1968).
13. A. S. Argon, I. W. Chen and C. W. Lau, Mechanics and mechanisms of intergranular cavitation in creeping alloys. In *Three-Dimensional Constitutive Relations and Ductile Fracture* (Edited by S. Nemat-Nasser), pp. 23–49. North-Holland, Amsterdam (1981).
14. A. Needleman and J. R. Rice, Limits to ductility set by plastic flow localization. In *Mech. Sheet Metal Forming* (Edited by D. Koiskinen *et al.*), pp. 237–267. Plenum, New York (1978).
15. P. S. Theocaris, Caustics in plane-strain: evaluation of COD and the core region. *Engng Fracture Mech.* **19**(1), 81–92 (1984).
16. A. S. Argon, J. Im and R. Safoglu, Cavity formation from inclusions in ductile fracture. *Metal. Trans.* **6A**, 825–837 (1975).
17. P. S. Theocaris, Elastic stress intensity factors evaluated by caustics. In *Experimental Determination of Crack Tip Stress Intensity Factors, Mechanics of Fracture* (Edited by G. C. Sih), Vol. VII, Chap. 3, pp. 189–252. Martinus Nijhoff, The Hague (1981).
18. P. S. Theocaris, Glassy polymers and photoelastic materials. *Int. J. Mech. Sci.* **18**(4), 171–178 (1976).

19. V. Nagpal, F. A. McClintock, C. A. Berg and M. Subudhi, Traction displacement boundary conditions for plastic fracture by hole growth. In *Proc. Int. Symp. on Foundations of Plasticity* (Edited by A. Sawczuk), Vol. 1, pp. 365–385.
20. A. S. Argon, *Relationships Between Structure and Mechanical Behavior in Polymeric Solids* (Edited by E. Baer and V. Radcliffe). ASM, Providence, RI (1973).
21. P. S. Theocaris, Yield criteria depending on pressure and dilatancy. *Proc. Natn. Acad. Athens* **58**(1), 428–453 (1983).
22. F. Schleicher, Die Energiegrenze der Elastizität (Plastizitätsbedingung). *Z. Angew. Math. Mech.* **5**, 478–479 (1925).
23. F. Stassi-D'Alia, Flow and fracture of materials according to a new limiting condition of yielding. *Mechanica* **3**(3), 178–195 (1967).
24. A. Nadai, *Theory of Flow and Fracture of Solids*. McGraw-Hill, New York (1950).
25. J. C. Bauwens, Deformation plastique des hauts Polymères vitreux soumis à un Système des Contraintes queleonque, *J. Polym. Sci. A-2* **5**, 1145–1156 (1967); see also **8**, 893–901 (1970).
26. S. S. Sternstein and L. Ongchin, Yield criteria for plastic deformation of glassy high polymers in general stress fields. *Am. Chem. Soc. Polym. Preprints* **10**(2), 1117–1124 (1969).
27. R. C. Grassi and I. Cornet, Fracture of gray-cast-iron tubes under biaxial stresses. *J. Appl. Mech. Trans. ASME* **16**(2), 178–182 (1949).
28. L. F. Coffin Jr., The flow and fracture of a brittle material. *J. Appl. Mech. Trans. ASME* **17**(3), 233–248 (1950).